J Mater Sci: Mater Electron (2024) 35:1497

Analysis of CeO_2/SiO_2 double-layer thin film stack with antireflection effect for silicon solar cells

Imran Kanmaz[1,*], Murat Tomakin[1], and Abdullah Uzum[2]

[1] *Faculty of Arts and Sciences, Department of Physics, Recep Tayyip Erdogan University, 53100 Rize, Türkiye*
[2] *Faculty of Engineering, Department of Electrical and Electronics Engineering, Karadeniz Technical University, 61080 Trabzon, Türkiye*

Received: 1 March 2024
Accepted: 20 July 2024

ABSTRACT

This study introduces CeO_2/SiO_2 double-layer film stacks and its antireflection coating effect. Optical properties were analyzed by spectrophotometer measurements; surface morphology and cross-sections were observed by Scanning Electron Microscopy (SEM); elemental distributions and crystallographic properties were determined by Energy Dispersive Spectroscopy (EDS) and X-ray Diffraction (XRD) measurements. Average reflectance of single-layer $0.3MSiO_2$, $0.6MSiO_2$, and $0.3MCeO_2$ thin films were 30.54%, 20.12%, and 14.23%, respectively. Average reflectance was decreased significantly down to 5.9% by $0.3MCeO_2/0.6MSiO_2$ double-layer thin films comparing to those of the results of single-layer films and bare silicon surface reflection (~40%). Antireflective effect of the films on solar cells was estimated by simulation using the measured reflection data. Simulated solar cells indicate that $0.3MCeO_2/0.6MSiO_2$ double-layer antireflective coatings are capable to increase the efficiency significantly and conversion efficiency of 21.7% could be achieved.

1 Introduction

Improving the absorption ratio of the photons has significant effect on the increasing of solar cell conversion efficiency. The reflected photons from the surface cannot contribute to the photovoltaic effect and are considered as a loss. Reflections on the surface of a solar cell can be minimized by employing an appropriate antireflection coating on the illuminated surface of the device. Additionally, advanced design techniques such as surface texturing are employed to improve light trapping and to achieve higher efficiency solar cells, aiming to minimize losses. Various materials such as TiO_2, HfO_2, Al_2O_3, CeO_2, SiN_x, ZnO, and SiO_2 are utilized as a single and double-layer antireflection coating films. Transparent conductive oxide thin film electrodes can act simultaneously as an antireflective layer as well [1]. Generally single-layer antireflection coatings (SLAR) are designed to achieve minimum reflection on a solar cell surface at a wavelength of 550 nm where the solar spectrum peaks. The refractive index (n) of these coatings typically ranges between 1.8 and 2.0, while the thickness (d) falls within the range of 60 to 70 nm [2]. Due to the limitations of SLAR

Address correspondence to E-mail: imrankanmaz@ktu.edu.tr
E-mail Addresses: murat.tomakin@erdogan.edu.tr; auzum@ktu.edu.tr

https://doi.org/10.1007/s10854-024-13245-5
Published online: 31 July 2024

coatings in covering a broad solar spectrum, investigations are going on for DLAR as well [3–5]. DLAR coatings are capable to provide lower average reflection over a broader wavelength range compared to SLAR coatings. The compatibility between the design and materials used in DLAR coatings is crucial for minimizing the reflection. For instance, materials with higher refractive indices (2.2 ~ 2.6) are preferred for the bottom layer of a DLAR coating where the lower refractive index materials (1.3 ~ 1.6) are used for the top layer of the coating [6] for sequential indexing for silicon substrates. SiO_2- and CeO_2-based thin films have not been studied in detail for the antireflection purposes yet. However, considering that the refractive indexes of SiO_2 and CeO_2 thin films are 1.56 and 2.20, respectively [7, 8], this stack can be an alternative for DLAR coatings.

Solution-based methods in thin film coatings are simpler and more economical compared to other coating techniques and are more useful and advantageous in industrial production because they contain non-hazardous precursors [9]. In this study, CeO_2/SiO_2 double-layer thin films were produced on crystalline silicon substrates using cost-effective and easy-to-apply spin coating method. Different precursors were prepared, and characterizations were carried out to show its potential as an alternative antireflection coating film. Introduced CeO_2/SiO_2 film stacks in this work can be an important contribution to the literature as an alternative set of double-layer antireflection coatings.

2 Materials and methods

Cerium (III) chloride heptahydrate ($CeCl_3.7H_2O$, 99% trace metals basis, Sigma-Aldrich) was utilized as the cerium source and ethyl alcohol was chosen as the solvent in the solution for CeO_2 thin films. Additionally, 0.2M citric acid monohydrate (Merck, 99.7%) was added to the mixed solution, and stirred for 5 min. The mixture underwent an aging process for 24 h. Then, 75 µl of triethanolamine (97%) was added and mixed at 50 °C to improve the adhesion between the film and substrate. The solution for the SiO_2 thin films was prepared by mixing TEOS ($C_8H_{20}O_4Si$-99%), ethyl alcohol, and deionized water in a ratio of 3:2:4 (in volume). Solutions with concentrations of 0.3 M and 0.6 M were prepared, and 25 µl of HCl acid was added to each solution. After obtaining a homogeneous mixture using a magnetic stirrer for half an hour, the solution was aged for 24 h. 725-µm-thick p-type crystalline silicon substrates (100) with the size of 1.5 × 1.5 cm were used as a substrate for reflectance measurements. The cleaning of the substrates was performed in three subsequent stages: immersion in diluted HF acid, ultrasonic bath in distilled water for 5 min, and then ultrasonic bath in ethyl alcohol for 5 min.

For optical measurements on glass, 1 × 1 cm quartz glass was used. Quartz glasses were cleaned with ethyl alcohol, acetone, and pure water for 5 min each, respectively. Coating of CeO_2 thin films was carried out at 6000 rpm for 20 s, while coating of SiO_2 thin films was carried out at 4000 rpm for 20 s [2, 10].

Formation of the CeO_2/SiO_2 double-layer films was carried out in two stages: preparation of solutions and formation of the films by spin coating, as shown in Fig. 1. CeO_2 thin films were spin coated first on the crystalline silicon substrates. To form CeO_2/SiO_2 double layer, SiO_2 thin films were deposited onto CeO_2 thin films at two different molarities of 0.3 M and 0.6 M. To form a compact CeO_2/SiO_2 double layer, CeO_2 film was coated on silicon substrate and annealed at 500 °C for 120 min. Then, SiO_2 film was coated on CeO_2 layer and annealed at 950 °C for 7 min.

Characterizations of the fabricated thin films were performed mainly by spectrophotometer measurements, Scanning Electron Microscopy (SEM) measurements, Energy Dispersive Spectroscopy (EDS) measurements, and X-ray Diffraction (XRD) measurements. The impact of CeO_2/SiO_2 DLAR antireflective coatings on the conversion efficiency of silicon solar cells was simulated by SCAPS.

3 Result and discussion

3.1 XRD patterns

XRD patterns measured at both 1° and 3° degrees for bare silicon (Si) are presented in Fig. 2a. As seen in the figure, the peaks at 1° are weaker and broader, indicating their association with crystalline silicon where the peaks at 3° are sharper and more distinct. XRD measurements were performed at 1° angles in each sample to minimize peaks originating from crystalline silicon and enhance the clarity of peaks of the thin film. The XRD patterns of CeO_2/SiO_2 thin films grown on crystalline silicon are given in Fig. 2b. When compared with the characteristics of CeO_2 SLAR thin films, it is observed that the peak intensities of CeO_2/SiO_2 DLAR

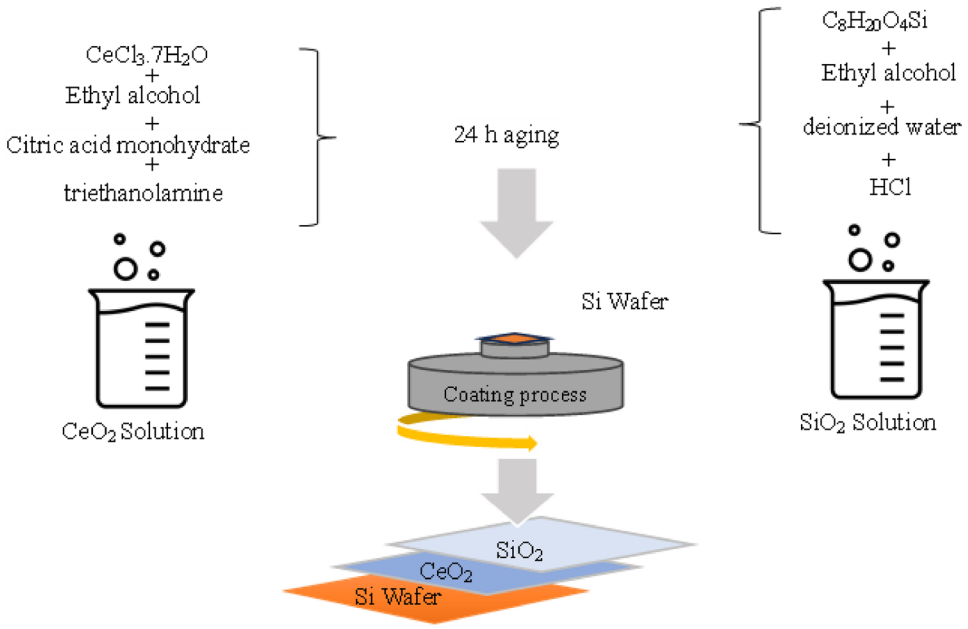

Fig. 1 Schematic representation of solution preparation and coating of CeO_2 and SiO_2 thin films

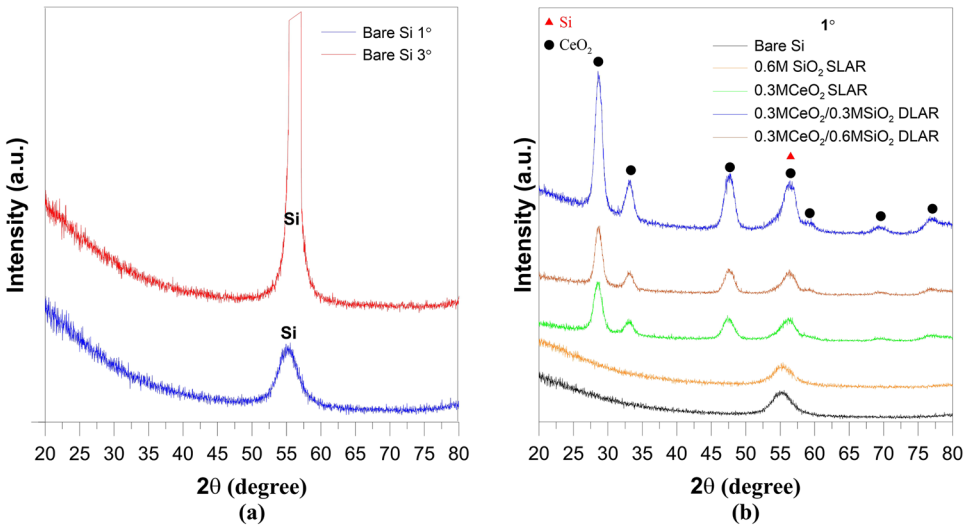

Fig. 2 XRD patterns of bare Si (**a**), CeO_2 SLAR and SiO_2/CeO_2 DLAR thin film (**b**)

thin films have significantly increased. Increased peak intensities can be due to the annealing of the SiO_2 thin film as the upper layer at a high temperature of 950 °C.

The elevated annealing temperature has led to a more pronounced appearance of CeO_2 peaks. Additionally, among the DLAR structures of 0.3M CeO_2/0.3M SiO_2 and 0.3M CeO_2/0.6M SiO_2, the bilayer structure of 0.3MCeO_2/0.3MSiO_2 demonstrated stronger peaks originating from CeO_2 thin films. This is attributed to the formation of a thicker SiO_2 thin film due to the higher molarity of SiO_2 in the 0.3M CeO_2/0.6M SiO_2 structure that could be able to suppress the CeO_2 peaks. As the crystallization of the SiO_2 cannot occur at 950°C, no related XRD peaks were observed [11]. The 0.3M CeO_2 SLAR thin film contains a total of four major peaks. The main peak of the CeO_2 thin film is positioned at 28.44°, and it is determined to grow on the (111) plane. Additionally, it possesses three major peaks at 32.96°, 47.42°, and 56.52°, growing on the (200), (202), and (311) planes, respectively. However, it is observed that the CeO_2 peak at 56.52° overlaps with the Si peak as shown in Fig. 2b. The peak characteristics of 0.3M CeO_2 SLAR on Fig. 2b are listed

Table 1 XRD peak parameters of CeO_2 thin film (Card No: 96-434-3162)

Peak no	2θ	(hkl)	FWHM	D (nm)	$\delta = 1/D^2$
1	28.44	111	1.1600	7.06	0.020
2	32.96	200	1.1000	7.53	0.017
3	47.42	202	1.6000	5.42	0.034
4	56.52	311	1.3200	6.83	0.021

in Table 1. The average crystal size (D) and dislocation density (δ) of the crystalline films based on X-ray diffraction patterns were calculated using the Debye–Scherrer equation (Eq. 1 and Eq. 2);

$$D = \frac{0.9\lambda}{\beta cos\theta} \tag{1}$$

$$\delta = \frac{1}{D^2}, \tag{2}$$

where λ is the wavelength, θ is the Bragg angle, and β is the half-peak width [12, 13].

The crystal size related to the main peak at 28.44° in the (111) plane is 7.06 nm which is in a good agreement with the literature [14]. The smallest crystal size was calculated to be 5.42 nm at an angle of 47.42°.

3.2 SEM images and EDS patterns

SEM measurements were conducted to observe the surface morphology of coated silicon substrates with SLAR and DLAR. SEM images of CeO_2 and SiO_2 SLAR coatings are presented in Fig. 3a, b. According to Fig. 3, both CeO_2 and SiO_2 thin films exhibit a homogeneous distribution. However, CeO_2 thin films display a more crack-prone structure compared to SiO_2 thin films. Cross-sectional images of CeO_2/SiO_2 DLAR are provided in Fig. 3c, d. SiO_2 thin film formation onto the CeO_2 thin film successfully filled the cracks on the surface, resulting in a more homogeneous thin film structure. Figure 3d reveals a two-layer structure in the cross-section of the thin films, with the SiO_2 thin film appearing thicker upper layer compared to the CeO_2 thin film. According to the cross-section measurements of CeO_2/SiO_2 DLAR thin films, the average thicknesses of CeO_2 and SiO_2 thin films are around 75 nm and 115 nm, respectively. Resulted thickness of the CeO_2/SiO_2 DLAR structure is 190 nm.

EDS micrographs of CeO_2/SiO_2 double-layer thin films are given in Fig. 4. Composition ratios of Si, Ce, and O are 55.3%, 21.4%, and 23.3%, respectively.

EDS results present higher ratio of Si compared to the ratio of other elements. This can be due to the presence of silicon as a substrate and the contribution by

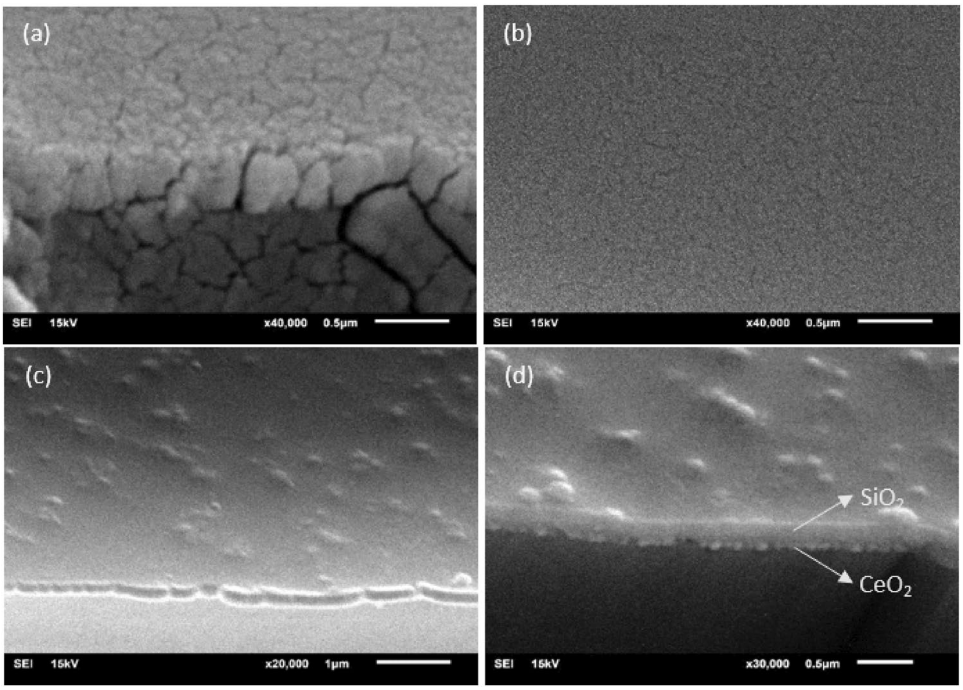

Fig. 3 SEM images of $0.3MCeO_2$ SLAR-coated surface (**a**), $0.6MSiO_2$ SLAR-coated surface (**b**), and $0.3MCeO_2/0.6MSiO_2$ DLAR coating cross-section (**c**, **d**)

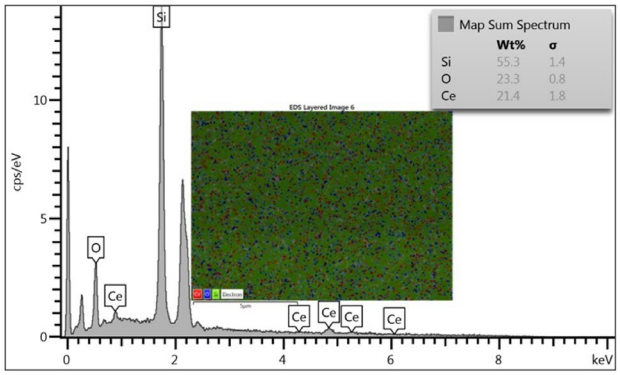

Fig. 4 EDS micrographs of double-layer CeO_2/SiO_2 thin films

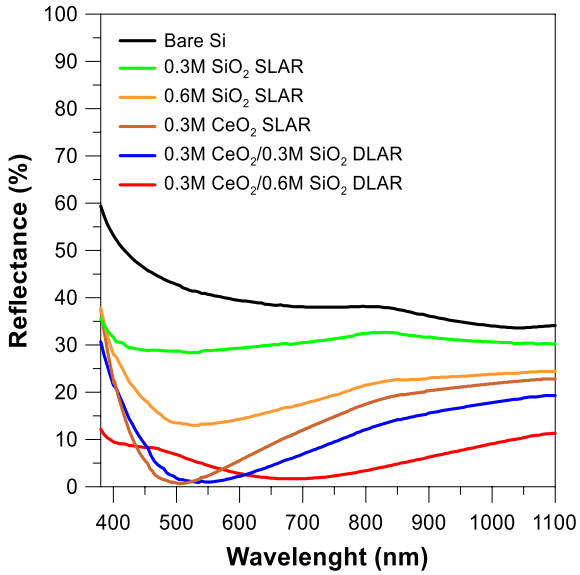

Fig. 5 Reflectance of bare silicon surface and SiO_2 SLAR, CeO_2 SLAR, and CeO_2/SiO_2 DLAR thin film coated surfaces

the coated SiO_2 thin films as a second layer. Besides, since the atomic number of Ce is higher than that of the Si and O, the X-rays coming to the surface may excite more to the Si atoms.

3.3 Optical properties

Minimizing the surface reflections is a key factor to improve the efficiency of crystalline silicon solar cells that can be achieved by using SLAR and DLAR coatings. In this part, the antireflective effects of SiO_2 and CeO_2 SLAR and CeO_2/SiO_2 DLAR thin films formed onto the crystalline silicon surface were investigated. Figure 5 presents the reflectance spectra of coated SLAR and DLAR thin films on silicon substrates. Average reflectance and minimum reflectance values for each structure are summarized in Table 2.

Average reflection of bare Si surface within the wavelength range of 380–1100 nm (Table 2) was 39.16%. Surface reflectance of the Si substrate coated with $0.3MSiO_2$, $0.6MSiO_2$, and $0.3MCeO_2$ thin films were 30.54%, 20.12%, and 14.23%, respectively. Further decrease of the reflectance could be confirmed on the DLAR-coated surfaces. For instance, when $0.3MSiO_2$ was coated on the $0.3MCeO_2$ thin film, the reflection decreased to down to 11.15%, representing a further reduction of approximately 3% compared to the single-layer $0.3MCeO_2$ thin film. Moreover, the average reflection decreased further to a value of 5.9% when $0.6MSiO_2$ was coated on the $0.3MCeO_2$ thin film. These results show that $0.3MCeO_2/0.6MSiO_2$ DLAR thin film provides approximately 33% and 9% lower reflection when comparing to that of the reflections on the bare Si and single-layer $0.3MCeO_2$ thin film coated surface, respectively.

These findings demonstrate that DLAR coatings are more effective than single-layer antireflection coatings as reported elsewhere [15, 16]. Specifically, SiO_2 thin films are highly effective in double-layer antireflection coatings and are commonly preferred as the top low refractive index layer [17, 18]. Additionally, transmittance and absorbance measurements of CeO_2 and SiO_2 SLAR thin films (Fig. 6a, b) were performed. As can be confirmed in Fig. 6a, $0.6MSiO_2$ thin films exhibit better transparency compared to $0.3MCeO_2$ thin films. Similarly, CeO_2 thin films demonstrate superior absorption characteristics as can be confirmed in Fig. 6 (b). Particularly in the wavelength range of 200–400 nm, significant absorption was observed in CeO_2 thin films.

Transmittance and absorbance of CeO_2/SiO_2 DLAR thin films are given in Fig. 7. The deposition of $0.3MSiO_2$ and $0.6MSiO_2$ thin films on top of $0.3MCeO_2$ thin film to form DLAR structure increased the transmittance and decreased the absorbance. For instance, the transmittance kink of $0.3MCeO_2$ SLAR thin film was at 350 nm (with transmittance of 80%), while the kink of $0.3MCeO_2/0.6MSiO_2$ DLAR thin film was observed at 450 nm (with transmittance of 98%). The average transmittance of those SLAR and DLAR layers were 66.6% and 78.6% in the range of 200–1000 nm, respectively.

Additionally, both $0.3MCeO_2/0.3MSiO_2$ and $0.3MCeO_2/0.6MSiO_2$ DLAR-coated thin films

Table 2 Reflectance data summary of SiO_2, CeO_2 SLAR, and CeO_2/SiO_2 DLAR thin films

Sample	R_{Ave}(%) (400–700nm)	R_{Ave}(%) (380–1100nm)	R_{Min} (%)	R_{Min} point (nm)
Bare Si	42.12	39.16	33.6	1043
0.3MSiO_2 SLAR	29.36	30.54	28.3	520
0.6MSiO_2 SLAR	16.26	20.12	13	530
0.3MCeO_2 SLAR	6.35	14.23	0.6	506
0.3MCeO_2/0.3MSiO_2 DLAR	5.33	11.15	0.9	535
0.3MCeO_2/0.6MSiO_2 DLAR	4.96	5.90	1.7	680

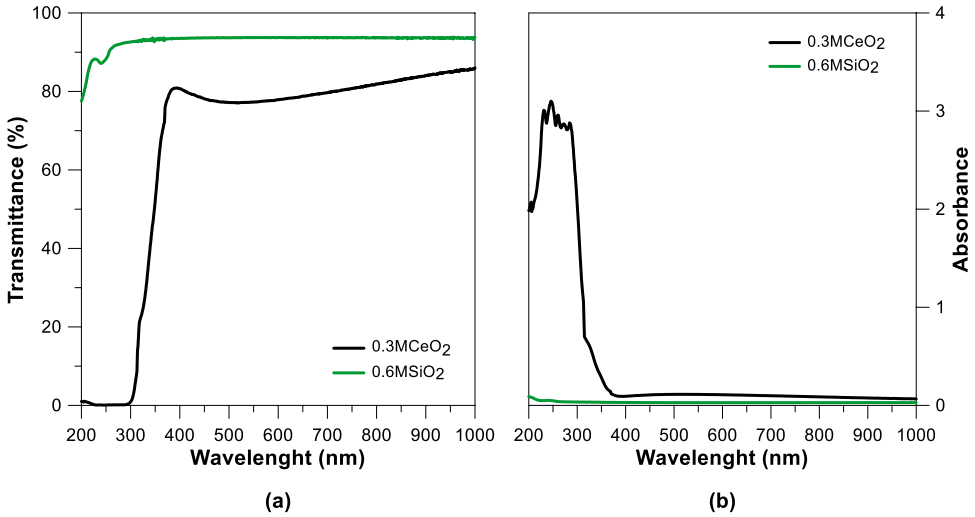

Fig. 6 Transmittance (**a**) and absorbance (**b**) of CeO_2 and SiO_2 SLAR layers

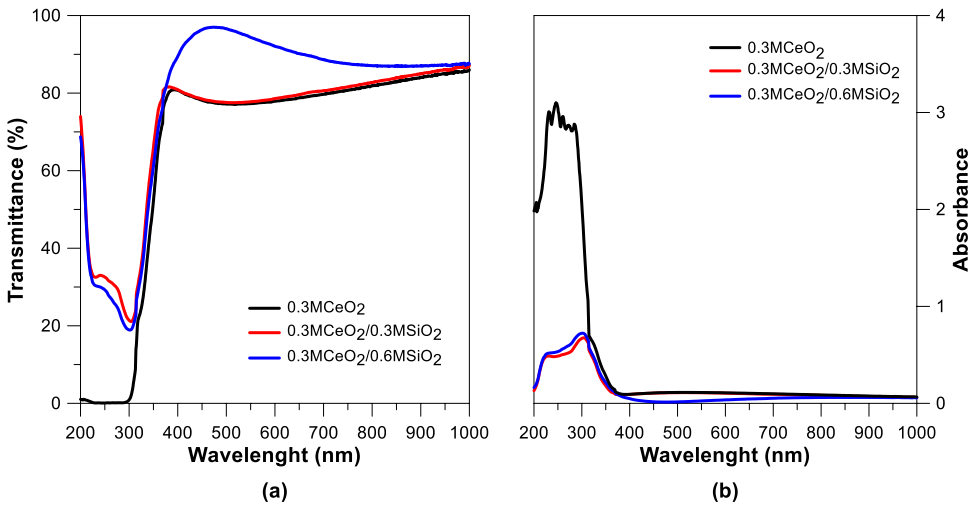

Fig. 7 Transmittance (**a**) and absorbance (**b**) of CeO_2/SiO_2 DLAR coating layer

exhibited an increase in transmittance of approximately 25% at low wavelengths (200–300 nm). These results indicate that CeO_2/SiO_2 DLAR coatings enhance optical properties, particularly leading to a significant increase in transmittance below 700 nm.

3.4 Solar cell structure and simulation results

The impact of SLAR and DLAR coatings on the conversion efficiency of crystalline silicon solar cells was assessed by a simulation study by SCAPS using

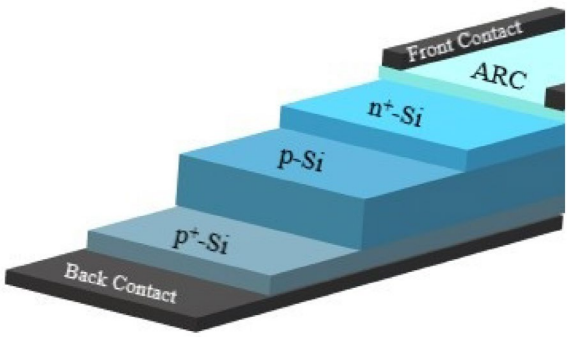

Fig. 8 Schematic representation of simulated conventional silicon solar cell

experimentally determined reflectance parameters. SCAPS is a one-dimensional simulation software offered to design solar cell structures such as heterojunctions and crystalline silicon. The program solves basic semiconductor equations based on the optical properties of the selected materials, simulating electrical parameters to analyze the performance of the solar cell comprehensively [19, 20]. Simulated solar cell structure is illustrated in Fig. 8, and the initial parameters of the solar cell are given in Table 3. Designed conventional silicon solar cell consists of a total of four layers, including back surface field (p^+-Si BSF), base (p-Si), emitter (n^+-Si), and antireflection coating.

A conventional silicon solar cell was simulated without an antireflection coating for comparison. Based on calculated solar cell parameters, a significant influence of the minimized reflection on the solar cell performance was observed. As summarized in Table 4, the efficiency of solar cell without an antireflection coating on the surface was 13.9%. High average reflection on the front surface decreases the current density and the conversion efficiency. The presence of antireflection coatings on solar cell surface, on the other hand, minimizes the reflection and increases the efficiency. For instance, solar cells with $0.3MSiO_2$, $0.6MSiO_2$, and $0.3MCeO_2$ SLAR thin films as an antireflection coating reach the efficiency of 15.9%, 18.4%, and 19.7%, respectively.

However, efficiency of the solar cells with $0.3MCeO_2/0.3MSiO_2$ DLAR and $0.3MCeO_2/0.6MSiO_2$ DLAR layers leads to higher efficiencies of 20.5% and 21.7%, respectively. Figure 9 shows the I–V characteristics of simulated solar cells where the increase of the short circuit current density (J_{sc}) owing to the antireflective effect of the coated layer could be clearly seen. The maximum J_{sc} of the solar cells with

Table 3 c-Si solar cell initial parameters [21, 22]

	p-Si	p^+-Si-BSF	n^+-Si
Thickness (μm)	200	7	0.3
Bandgap (eV)	1.12	1.12	1.12
Electron affinity (eV)	4.05	4.05	4.50
Dielectric permittivity	11.90	11.90	11.90
CB effective density of states (cm^{-3})	2.80×10^{19}	2.80×10^{19}	2.80×10^{19}
VB effective density of states (cm^{-3})	1.04×10^{19}	1.04×10^{19}	1.04×10^{19}
Electron mobility (cm^2/Vs)	1041	202	1350
Hole mobility (cm^2/Vs)	412	77	480
Shallow uniform donor density N_D (cm^{-3})	1×10^{16}	0	1×10^{20}
Shallow uniform acceptor density N_A (cm^{-3})	1×10^{17}	1×10^{19}	0

Table 4 Parameters of solar cells using different antireflective coatings

	V_{oc} (V)	J_{sc} (mA/cm^2)	FF (%)	η (%)
non-ARC	0.733	23.50	80.34	13.9
$0.3MSiO_2$ SLAR	0.737	26.83	80.33	15.9
$0.6MSiO_2$ SLAR	0.740	30.86	80.24	18.4
$0.3MCeO_2$ SLAR	0.742	33.13	80.15	19.7
$0.3MCeO_2/0.3MSiO_2$ DLAR	0.743	34.32	80.11	20.5
$0.3MCeO_2/0.6MSiO_2$ DLAR	0.745	36.35	80.01	21.7

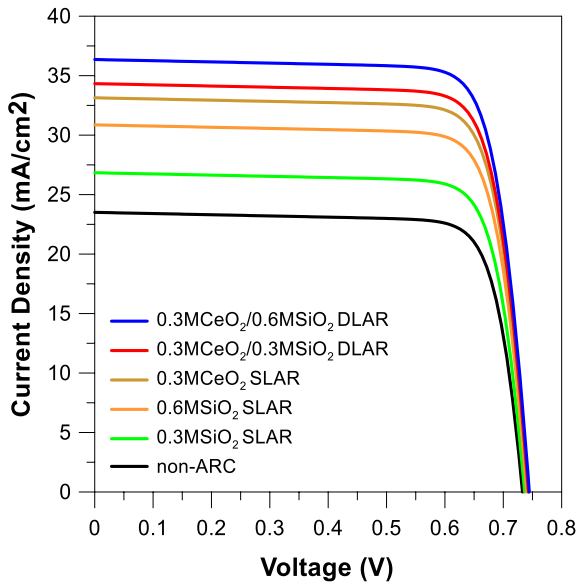

Fig. 9 I–V characteristics of solar cells with different antireflective coatings

SLAR coatings was 33.13 mA/cm^2, obtained by the effect of 0.3MCeO$_2$ SLAR coating. J_{sc} of the solar cells could be increased further by 0.3MCeO$_2$/0.3MSiO$_2$ DLAR and 0.3MCeO$_2$/0.6MSiO$_2$ DLAR coatings to 34.32 and 36.35 mA/cm^2, respectively. These results clearly demonstrate the effectiveness of double-layer antireflection coatings to enhance the efficiency of solar cells owing to the minimized reflection on the illuminated surface.

4 Conclusions

CeO$_2$/SiO$_2$ DLAR coatings were introduced in this study by simple and cost-effective spin coating technique. Optical performances of such films were compared with CeO$_2$ and SiO$_2$ SLAR coatings and with bare silicon surface. 0.3MSiO$_2$, 0.6MSiO$_2$, and 0.3MCeO$_2$ SLAR coatings and 0.3MCeO$_2$/0.3MSiO$_2$ DLAR and 0.3MCeO$_2$/0.6MSiO$_2$ DLAR coatings were analyzed. 0.3MCeO$_2$/0.6MSiO$_2$ DLAR films reduce the reflectance down to 5.9% when coated on the silicon substrate. The impact of these coatings on the conversion efficiency of crystalline silicon solar cells was estimated through simulation using SCAPS software. The results indicated a substantial improvement in efficiency for solar cells with CeO$_2$/SiO$_2$ DLAR coatings compared to those of uncoated and SLAR-coated cells. The DLAR structure improves the solar cell performance by achieving a maximum efficiency of 21.7% owing to the significant increase in current density. In conclusion, this study successfully demonstrated CeO$_2$/SiO$_2$ DLAR thin films as an effective alternative antireflection coating for silicon substrates.

Acknowledgements

This study was supported by Scientific and Technological Research Council of Turkey (TUBITAK) under the Grant Number 121C375. The authors thank to TUBITAK for their supports. Authors also thank to Recep Tayyip Erdogan University faculty of engineering and architecture Thin Film Laboratory, where the thin films were produced.

Author contributions

Kanmaz, I contributed toward conceptualization, formal Analysis, investigation, methodology, project administration, resources, supervision, validation, visualization, writing-original draft, and writing–review and editing. Tomakin, M contributed toward supervision, conceptualization, validation, visualization, investigation, and resources. Uzum, A contributed toward writing–review and editing, resources, conceptualization, validation, and visualization.

Funding

Open access funding provided by the Scientific and Technological Research Council of Türkiye (TÜBİTAK).

Data availability

Data will be made available on request.

Declarations

Conflicts of interest The authors declared that they have no conflicts of interest to this work.

References

1. G.T. Chavan, Y. Kim, M.Q. Khokhar, S.Q. Hussain, E.-C. Cho, J. Yi, Z. Ahmad, P. Rosaiah, C.-W. Jeon, Nanomaterials **13**, 1226 (2023). https://doi.org/10.3390/nano13071226
2. İ Kanmaz, M. Tomakin, J. Sol-Gel Sci. Technol. **108**, 361–367 (2023). https://doi.org/10.1007/s10971-023-06161-3
3. S. Zeyed, A.N. AbdAlgaffar, Iraqi J. Phys. **21**, 25–32 (2023). https://doi.org/10.30723/ijp.v21i2.1110
4. A.S. Rad, A. Afshar, M. Azadeh, Opt. Mater. **136**, 113501 (2023). https://doi.org/10.1016/j.optmat.2023.113501
5. M.A. Zahid, M.Q. Khokhar, S. Park, S.Q. Hussain, Y. Kim, J. Yi, Vacuum **200**, 110967 (2022). https://doi.org/10.1016/j.vacuum.2022.110967
6. I. Lee, D. Lim, S. Lee, J. Yi, Surf. Coat. Technol. **137**, 86–91 (2001). https://doi.org/10.1016/S0257-8972(00)01076-8
7. A. Hashim, M. Abbas, N.A.-H. Al-Aaraji, A. Hadi, J. Inorg. Organomet. Polym. Mater. **33**, 1–9 (2023). https://doi.org/10.1007/s10904-022-02485-9
8. K. Ali, S.A. Khan, M.M. Jafri, Int. J. Electrochem. Sci. **9**, 7865–7874 (2014). https://doi.org/10.1016/S1452-3981(23)11011-X
9. G. Chavan, F. Sabah, S. Kamble, V. Prakshale, S. Pawar, S. Patil, S. Lee, A. Sikora, L. Deshmukh, Y. Cho, Ceram. Int. **46**, 74–80 (2020). https://doi.org/10.1016/j.ceramint.2019.08.235
10. I. Kanmaz, Ü. Abdullah, Int. Adv. Res. Eng. J. **5**, 14–18 (2021). https://doi.org/10.35860/iarej.784328
11. Y. Liu, W. Ren, L. Zhang, X. Yao, Thin Solid Films **353**, 124–128 (1999). https://doi.org/10.1016/S0040-6090(99)00419-8
12. D.S. Kim, S.J. Han, S.-Y. Kwak, J. Colloid Interface Sci. **316**, 85–91 (2007). https://doi.org/10.1016/j.jcis.2007.07.037
13. R. Suresh, V. Ponnuswamy, R. Mariappan, N.S. Kumar, Ceram. Int. **40**, 437–445 (2014). https://doi.org/10.1016/j.ceramint.2013.06.020
14. J. Zimou, K. Nouneh, R. Hsissou, A. El-Habib, L. El Gana, A. Talbi, M. Beraich, N. Lotfi, M. Addou, Mater. Sci. Semicond. Process. **135**, 106049 (2021). https://doi.org/10.1016/j.mssp.2021.106049
15. A.K. Saini, A. Singh, V.S. Meena, S.K. Gaur, R. Pal, Mater. Sci. Semicond. Process. **147**, 106749 (2022). https://doi.org/10.1016/j.mssp.2022.106749
16. C. Ji, W. Liu, Y. Bao, X. Chen, G. Yang, B. Wei, F. Yang, X. Wang, Recent applications of antireflection coatings in solar cells. Photonics **9**, 906 (2022). https://doi.org/10.3390/photonics9120906
17. T. Sertel, Y. Ozen, V. Baran, S. Ozcelik, J. Alloy. Compd. **806**, 439–450 (2019). https://doi.org/10.1016/j.jallcom.2019.07.257
18. R. Sharma, Int. J. (2021). https://doi.org/10.30534/ijeter/2021/059102021
19. S. Karthick, S. Velumani, J. Bouclé, Opt. Mater. **126**, 112250 (2022). https://doi.org/10.1016/j.optmat.2022.112250
20. M. Burgelman, P. Nollet, S. Degrave, Thin Solid Films **361**, 527–532 (2000). https://doi.org/10.1016/S0040-6090(99)00825-1
21. K. Kim, J. Gwak, S.K. Ahn, Y.-J. Eo, J.H. Park, J.-S. Cho, M.G. Kang, H.-E. Song, J.H. Yun, Sol. Energy **145**, 52–58 (2017). https://doi.org/10.1016/j.solener.2017.01.031
22. R. Rasool, A.A. Mohammed, R.F. Hasan, Iraqi J Sci (2021). https://doi.org/10.24996/ijs.2021.62.5.16